Compact ultrafast semiconductor disk laser: targeting GFP based nonlinear applications in living organisms

Rodrigo Aviles-Espinosa,[1] George Filippidis,[2] Craig Hamilton,[3,4] Graeme Malcolm,[3] Kurt J. Weingarten,[5] Thomas Südmeyer,[6] Yohan Barbarin,[6] Ursula Keller,[6] Susana I.C.O Santos,[1] David Artigas,[1,7] and Pablo Loza-Alvarez[1,*]

[1]*ICFO - The Institute of Photonic Sciences, Mediterranean Technology Park, Av. Canal Olimpic s/n, 08860 Castelldefels (Barcelona), Spain*
[2]*Institute of Electronic Structure and Laser, Foundation of Research and Technology-Hellas, P.O. Box 1385, 71110 Heraklion, Crete, Greece*
[3]*M Squared Lasers Ltd, 1 Technology Terrace, Todd Campus, West of Scotland Science Park Maryhill Road, Glasgow G20 0XA, Scotland, UK*
[4]*Solus Technologies Limited, 1 Technology Terrace, Todd Campus, West of Scotland Science Park, Maryhill Road, Glasgow G20 0XA, Scotland, UK*
[5]*Time-Bandwidth-Products, Technoparkstr. 1, 8005, Switzerland*
[6]*Department of Physics, Institute of Quantum Electronics, ETH Zurich, 8093 Zurich, Switzerland*
[7]*Department of signal theory and communications, Universitat Politècnica de Catalunya, 08034 Barcelona, Spain*
**pablo.loza@icfo.es*

Abstract: We present a portable ultrafast Semiconductor Disk Laser (SDL) (or vertical extended cavity surface emitting laser—VECSELs), to be used for nonlinear microscopy. The SDL is modelocked using a quantum-dot semiconductor saturable absorber mirror (SESAM), delivering an average output power of 287 mW, with 1.5 ps pulses at 500 MHz and a central wavelength of 965 nm. Specifically, despite the fact of having long pulses and high repetition rates, we demonstrate the potential of this laser for Two-Photon Excited Fluorescence (TPEF) imaging of *in vivo Caenorhabditis elegans (C. elegans)* expressing Green Fluorescent Protein (GFP) in a set of neuronal processes and cell bodies. Efficient TPEF imaging is achieved due to the fact that this wavelength matches the peak of the two-photon action cross section of this widely used fluorescent marker. The SDL extended versatility is shown by presenting Second Harmonic Generation images of pharynx, uterus, body wall muscles and its potential to be used to excite other different commercial dyes. Importantly this non-expensive, turn-key, compact laser system could be used as a platform to develop portable nonlinear bio-imaging devices.

OCIS codes: (180.4315) Nonlinear microscopy; (190.4180) Multiphoton processes; (180.6900) Three-dimensional microscopy; (170.3880) Medical and biological imaging; (140.3538) Lasers, pulsed; (140.5960) Semiconductor lasers

References and links

1. W. Denk, J. H. Strickler, and W. W. Webb, "Two-photon laser scanning fluorescence microscopy," Science **248**(4951), 73–76 (1990).
2. C. Xu, W. Zipfel, J. B. Shear, R. M. Williams, and W. W. Webb, "Multiphoton fluorescence excitation: new spectral windows for biological nonlinear microscopy," Proc. Natl. Acad. Sci. U.S.A. **93**(20), 10763–10768 (1996).
3. U. Keller, "Recent developments in compact ultrafast lasers," Nature **424**(6950), 831–838 (2003).
4. U. Keller, "Ultrafast solid-state lasers," in *Landolt-Börnstein. Laser Physics and Applications. Subvolume B: Laser Systems. Part I*, G. Herziger, H. Weber, and R. Proprawe, eds. (Springer Verlag, Heidelberg, 2007), pp. 33–167
5. D. Kopf, K. J. Weingarten, L. R. Brovelli, M. Kamp, and U. Keller, "Diode-pumped 100-fs passively mode-locked Cr:LiSAF laser with an antiresonant Fabry-Perot saturable absorber," Opt. Lett. **19**(24), 2143–2145 (1994).

#139905 - $15.00 USD Received 21 Dec 2010; revised 23 Feb 2011; accepted 24 Feb 2011; published 28 Feb 2011

6. D. Kopf, K. J. Weingarten, G. Zhang, M. Moser, M. A. Emanuel, R. J. Beach, J. A. Skidmore, and U. Keller, "High-average-power diode-pumped femtosecond Cr:LiSAF lasers," Appl. Phys. B **65**(2), 235–243 (1997).
7. D. Kopf, G. Zhang, R. Fluck, M. Moser, and U. Keller, "All-in-one dispersion-compensating saturable absorber mirror for compact femtosecond laser sources," Opt. Lett. **21**(7), 486–488 (1996).
8. K. Svoboda, W. Denk, W. H. Knox, and S. Tsuda, "Two-photon-excitation scanning microscopy of living neurons with a saturable Bragg reflector mode-locked diode-pumped Cr:LiSrAlFl laser," Opt. Lett. **21**(17), 1411–1413 (1996).
9. J. M. Girkin and G. McConnell, "Advances in laser sources for confocal and multiphoton microscopy," Microsc. Res. Tech. **67**(1), 8–14 (2005).
10. S. Sakadžic, U. Demirbas, T. R. Mempel, A. Moore, S. Ruvinskaya, D. A. Boas, A. Sennaroglu, F. X. Kaertner, and J. G. Fujimoto, "Multi-photon microscopy with a low-cost and highly efficient Cr:LiCAF laser," Opt. Express **16**(25), 20848–20863 (2008).
11. G. Robertson, D. Armstrong, M. J. P. Dymott, A. I. Ferguson, and G. L. Hogg, "Two-photon fluorescence microscopy with a diode-pumped Cr:LiSAF laser," Appl. Opt. **36**(12), 2481–2483 (1997).
12. R. Aviles-Espinosa, S. I. Santos, A. Brodschelm, W. G. Kaenders, C. Alonso-Ortega, D. Artigas, and P. Loza-Alvarez, "Third-harmonic generation for the study of *Caenorhabditis elegans* embryogenesis," J. Biomed. Opt. **15**(4), 046020 (2010).
13. S. Tang, J. Liu, T. B. Krasieva, Z. P. Chen, and B. J. Tromberg, "Developing compact multiphoton systems using femtosecond fiber lasers," J. Biomed. Opt. **14**(3), 030508 (2009).
14. A. C. Millard, P. W. Wiseman, D. N. Fittinghoff, K. R. Wilson, J. A. Squier, and M. Müller, "Third-harmonic generation microscopy by use of a compact, femtosecond fiber laser source," Appl. Opt. **38**(36), 7393–7397 (1999).
15. M. Kuramoto, N. Kitajima, H. C. Guo, Y. Furushima, M. Ikeda, and H. Yokoyama, "Two-photon fluorescence bioimaging with an all-semiconductor laser picosecond pulse source," Opt. Lett. **32**(18), 2726–2728 (2007).
16. K. Taira, T. Hashimoto, and H. Yokoyama, "Two-photon fluorescence imaging with a pulse source based on a 980-nm gain-switched laser diode," Opt. Express **15**(5), 2454–2458 (2007).
17. H. Yokoyama, H. C. Guo, T. Yoda, K. Takashima, K. Sato, H. Taniguchi, and H. Ito, "Two-photon bioimaging with picosecond optical pulses from a semiconductor laser," Opt. Express **14**(8), 3467–3471 (2006).
18. H. J. Koester, D. Baur, R. Uhl, and S. W. Hell, "Ca2+ fluorescence imaging with pico- and femtosecond two-photon excitation: signal and photodamage," Biophys. J. **77**(4), 2226–2236 (1999).
19. K. König, T. W. Becker, P. Fischer, I. Riemann, and K. J. Halbhuber, "Pulse-length dependence of cellular response to intense near-infrared laser pulses in multiphoton microscopes," Opt. Lett. **24**(2), 113–115 (1999).
20. U. Keller and A. C. Tropper, "Passively modelocked surface-emitting semiconductor lasers," Phys. Rep. **429**(2), 67–120 (2006).
21. A. McWilliam, A. A. Lagatsky, C. T. A. Brown, W. Sibbett, A. E. Zhukov, V. M. Ustinov, A. P. Vasil'ev, and E. U. Rafailov, "Quantum-dot-based saturable absorber for femtosecond mode-locked operation of a solid-state laser," Opt. Lett. **31**(10), 1444–1446 (2006).
22. U. Keller, K. J. Weingarten, F. X. Kartner, D. Kopf, B. Braun, I. D. Jung, R. Fluck, C. Honninger, N. Matuschek, and J. Aus der Au, "Semiconductor saturable absorber mirrors (SESAM's) for femtosecond to nanosecond pulse generation in solid-state lasers," IEEE J. Sel. Top. Quantum Electron. **2**(3), 435–453 (1996).
23. D. J. Maas, A. R. Bellancourt, M. Hoffmann, B. Rudin, Y. Barbarin, M. Golling, T. Südmeyer, and U. Keller, "Growth parameter optimization for fast quantum dot SESAMs," Opt. Express **16**(23), 18646–18656 (2008).
24. E. Spiess, F. Bestvater, A. Heckel-Pompey, K. Toth, M. Hacker, G. Stobrawa, T. Feurer, C. Wotzlaw, U. Berchner-Pfannschmidt, T. Porwol, and H. Acker, "Two-photon excitation and emission spectra of the green fluorescent protein variants ECFP, EGFP and EYFP," J. Microsc. **217**(3), 200–204 (2005).
25. G. A. Blab, P. H. M. Lommerse, L. Cognet, G. S. Harms, and T. Schmidt, "Two-photon excitation action cross-sections of the autofluorescent proteins," Chem. Phys. Lett. **350**(1-2), 71–77 (2001).
26. R. Heim, A. B. Cubitt, and R. Y. Tsien, "Improved green fluorescence," Nature **373**(6516), 663–664 (1995).
27. Developmental Recourse for Biophysical Imaging Optoelectronics, "Two photon action cross sections" (Cornel University, 2010), http://www.drbio.cornell.edu/cross_sections.html
28. I. A. Hope, *C. elegans a Practical Approach* (Oxford University Press, 1999), Chap. 2.
29. Education in Microscopy and Digital Imaging, "Suitable dyes for multi-photon" (Zeiss virtual campus 2011), http://www.zeiss.com/C12567BE00472A5C/EmbedTitelIntern/MultiphotonSuitableDyes/$File/MultiphotonSuitableDyes.pdf
30. S. Psilodimitrakopoulos, V. Petegnief, G. Soria, I. Amat-Roldan, D. Artigas, A. M. Planas, and P. Loza-Alvarez, "Estimation of the effective orientation of the SHG source in primary cortical neurons," Opt. Express **17**(16), 14418–14425 (2009).
31. T. R. Neu, U. Kuhlicke, and J. R. Lawrence, "Assessment of fluorochromes for two-photon laser scanning microscopy of biofilms," Appl. Environ. Microbiol. **68**(2), 901–909 (2002).
32. B. J. Baker, H. Mutoh, D. Dimitrov, W. Akemann, A. Perron, Y. Iwamoto, L. Jin, L. B. Cohen, E. Y. Isacoff, V. A. Pieribone, T. Hughes, and T. Knöpfel, "Genetically encoded fluorescent sensors of membrane potential," Brain Cell Biol. **36**(1-4), 53–67 (2008).
33. A. Khatchatouriants, A. Lewis, Z. Rothman, L. Loew, and M. Treinin, "GFP is a selective non-linear optical sensor of electrophysiological processes in *Caenorhabditis elegans*," Biophys. J. **79**(5), 2345–2352 (2000).
34. J. White and E. Stelzer, "Photobleaching GFP reveals protein dynamics inside live cells," Trends Cell Biol. **9**(2), 61–65 (1999).

#139905 - $15.00 USD Received 21 Dec 2010; revised 23 Feb 2011; accepted 24 Feb 2011; published 28 Feb 2011

35. M. Mathew, S. I. C. O. Santos, D. Zalvidea, and P. Loza-Alvarez, "Multimodal optical workstation for simultaneous linear, nonlinear microscopy and nanomanipulation: upgrading a commercial confocal inverted microscope," Rev. Sci. Instrum. **80**(7), 073701 (2009).

1. Introduction

Nonlinear microscopy (NLM) techniques, such as Two-Photon Excited Fluorescence (TPEF) and Second Harmonic Generation (SHG), are able to overcome some of the drawbacks present on conventional Confocal Laser Scanning Microscopy (CLSM) [1,2]. This is in part due to the fact that the nonlinear excitation is confined to a focused volume rather than the whole illuminated beam path as it is the case for one-photon fluorescence. Therefore photo-toxicity and out of focus photo-bleaching are considerably decreased. This confinement of light is advantageous since it allows optical sectioning of the sample, enabling the reconstruction of three dimensional (3D) models. In addition, nonlinear excitation normally relies on the use of wavelengths in the near-infrared (NIR) range. At these wavelengths, besides the fact that there is reduced photo damage, Rayleigh scattering is also decreased enabling larger penetration depths.

A key element in a nonlinear microscope is the use of an ultrafast laser. These are natural sources that are able to produce the required high intensities needed for exciting nonlinear processes. Historically, Ti:sapphire sources have been used in NLM due to its available large peak powers along with its large tunability range. However, its complexity, high price and maintenance requirements, have limited the widespread adoption of these powerful imaging techniques into daily routine biomedical applications.

Efforts in the past have explored developing compact, lower-cost, and easy to use ultrafast semiconductor saturable absorber mirrors (SESAM) for modelocking diode-pumped solid-state lasers [3,4]. Compact designs can be realized by "folding" long cavities using careful mechanical design, or by increasing the repetition rate of the lasers which naturally allows short cavity lengths. However these sources have been limited by the available peak powers. More recently, compact ultrafast Cr-doped laser systems such as Cr:LiCAF, Cr:LiSAF, Cr:LiSGAF, lasers [4–6] (see Ref [4], Table. 2.1.2 for an overview on these sources) have been produced. Some of these have been employed for nonlinear TPEF imaging [7–11] and although average powers of up to 500mW have been demonstrated [6], they are often limited in their ability to sufficiently scale their average power.

Other alternative sources based on fiber lasers [12–14] and semiconductor laser diodes with amplification schemes [15–17] have also been successfully demonstrated as compact lasers for NLM applications. Fiber lasers can generate very short pulses via passive mode-locking, however, they are limited to wavelengths around 1030 nm and 1550 nm. In semiconductor lasers with amplification schemes, i.e., gain-switched laser source based on vertical cavity surface emitting lasers (VCSELs) [16], gain-switched InGaAsP Distributed-Feedback-Bragg (DFB), laser diode [17] and an external cavity mode-locked laser diode consisting of multiple quantum wells (AlGaAs) [15], the simplicity and compactness of these systems is compromised, as they need several stages to compress and/or amplify the pulses.

One key aspect for optimizing a compact laser for TPEF or SHG microcopy is the critical trade-off between repetition rate of the laser and the multiphoton signal strength generated [18, 19]. The signal strength in TPEF or SHG imaging scales as the product of the peak power times the average power (assuming image spot size, absorption, sample, detection path, etc. remain constant). This two-photon figure of merit (FOM_{2p}) allows one to make relative comparisons of laser sources as a function of their average power, pulse duration, and repetition rate (since peak power equals average power divided by repetition rate divided by pulse dlocking howeveruration). Typical Ti:sapphire lasers on a TPEF sample give a peak-power-average-power product (FOM_{2p}) of approximately 1 W^2 (e.g. 200 fs pulse duration, 80 MHz repetition rate, and 4 mW average power at the sample). Alternative laser sources should have a FOM_{2p} value of a similar order of magnitude. Higher repetition rate lasers allow for more compact designs, but require higher average power to achieve the same FOM_{2p} value.

#139905 - $15.00 USD Received 21 Dec 2010; revised 23 Feb 2011; accepted 24 Feb 2011; published 28 Feb 2011

Repetition rates in the multi-Gigahertz range have been demonstrated in TPEF imaging, but ultimately require average powers that begin to impact sample viability.

Here we experimentally show, for the first time, that an ultrashort pulse semiconductor disk laser (SDL) or vertical extended cavity surface emitting laser (VECSEL) that is modelocked by a "quantum dot-engineered" SESAM [20] can be in fact used for nonlinear microscopy. In fact, SDLs provide a compelling source for TPEF and SHG, as they combine key features such as excellent beam quality, output power, short pulse durations, amplitude stability, and can be made to operate at a large set of wavelengths, well-matched to key TPEF dyes, while maintaining simplicity and ease of operation. In addition, the repetition rate of these lasers can be adjusted into the 100's of MHz to 1 GHz, resulting in a compact laser cavity, but still working in a range where the FOM_{2p} can be reasonable (compared to the standard Ti:sapphire laser) without requiring excessively large average powers. SDL's also have the potential for low-cost manufacturing, as their gain element is based on wafer technology and because they have a relatively simple laser cavity design requiring only relatively low-cost and low-brightness pump diodes. Thus, in this work, we demonstrate the use of a modelocked VECSEL [20], with a footprint of only 140x240x70 mm, for *in vivo* multiphoton microscopy. The VECSEL gain chip is mode-locked with a quantum-dot SESAM [21–23] to produce 1.5 ps pulses at 500 MHz with an output average power of 287 mW at 965 nm. Importantly the laser output wavelength brings the advantage that TPEF of the Green Fluorescent Protein (GFP), one of the most widely used fluorescent markers for biological applications, has its two-photon action cross section maxima around this operating wavelength [2, 24–27]. Exciting the GFP at this wavelength substantially relaxes the required FOM_{2p} and corresponding average and peak power values needed for TPEF-based imaging. This is demonstrated in both, fixed samples and *in vivo* by imaging prepared slides containing different dyes and *Caenorhabditis elegans (C. elegans)* nematodes expressing GFP in a specific set of motoneurons respectively. In addition, the extended versatility of the laser is shown by presenting SHG images of pharynx, uterus and body wall muscles, followed by a demonstration of the ability of this source to excite various commercially available dyes.

The successful implementation of this non-expensive, maintenance-free, turn-key, compact laser system in a wide range of biological applications based on different markers and SHG could potentially facilitate the wide-spread adoption of nonlinear imaging techniques for "real-life" applications.

2. Materials and Methods

2.1. Experimental setup

The experimental setup shown in Fig. 1 was based on an inverted microscope (Nikon, Eclipse TE 2000U) modified to work as a laser scanning nonlinear microscope. A modelocked VECSEL (M Squared Lasers) operating at a central wavelength of 965 nm and having pulse duration of 1.5 ps and a repetition rate of 500 MHz was employed. The laser source geometry is the typical V-shaped cavity centered on the VECSEL chip mounted on a heat sink. The pump beam of this laser is focused at an angle of 45 degrees towards the VECSEL. A quantum-dot SESAM and a curved output coupling mirror form the end-mirrors of the laser cavity. To operate this laser, a simple web-based interface accessed through a PC was used to switch on the laser emission. The delivered output average power is of 287 mW corresponding to 0.4 KW peak power.

The microscope is equipped with a pair of x-y galvanometric mirrors (GM) (Cambridge technology, 6215H) used to scan the excitation beam over the sample. A telescope was used to adjust the fundamental beam diameter to fill the back aperture of the microscope objective. A filter cube, containing a hot mirror (Semrock, Inc., FF670-SDi01 transmittance = 360 nm – 650 nm reflectance = 680 nm – 1080 nm) and a BG39 band pass filter were used to separate the excitation beam from the generated TPEF signal. A 40x oil immersion microscope objective with NA = 1.3, (Nikon, Plan Fluor) was used during the experiments. The SHG signal was collected by an oil immersion condenser NA = 1.4, (Nikon). A custom made

#139905 - $15.00 USD Received 21 Dec 2010; revised 23 Feb 2011; accepted 24 Feb 2011; published 28 Feb 2011

forward detection mount with an attached photomultiplier tube (PMT) (Hamamatsu, H9305-04), and a band pass filter (transmittance = 475 - 485 nm) was employed to detect the SHG signal. To detect the TPEF emission a PMT (Hamamatsu, H9305-04), was mounted on one of the microscope ports. A custom made LabView interface was used to control both scanning units and the data acquisition card. The acquired *in vivo* images were volume rendered to allow for the 3D reconstruction employing Image J software. This procedure was repeated for the different samples for further analysis.

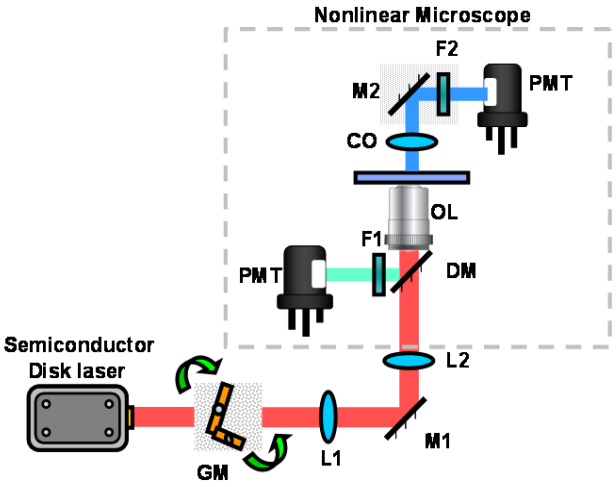

Fig. 1. Schematic experimental setup used for nonlinear imaging. The red path corresponds to the fundamental excitation beam centered at 965nm, the blue path to the SHG emission and the green path to the TPEF emission. L# are lenses; GM are the galvanometric mirrors; OL is the objective lens (40x, NA = 1.3), CO is the condenser optics (NA = 1.4); F_1 ad F_2 are the band pass filters (F_1 transmittance = 330 – 670 nm and F_2 transmittance = 475 – 485 nm); and PMT are the photo multiplier tubes.

2.2. Biological sample and fluorescent dyes

A set of fixed samples were employed for testing the imaging capabilities of the laser system. These were 1µm fluorescent beads (Duke Scientific G0100) containing green fluorescing firefly dye and a fixed sample containing a mouse intestine section (Invitrogen fluo cells slide #4 F-24631). This slide contained a combination of 3 dyes: Alexa Fluor 350 to mark the mucus of goblet cells, Alexa Fluor 568 phalloidin to label the filamentous actin prevalent in the brush border and SYTOX Green nucleic acid stain to label the nuclei of goblet cells.

The dyes employed for TPEF excitation/emission measurements were prepared in a solution. These were JC-1 (Invitrogen T-3168), Fluorescein (FD70 Sigma-Aldrich) and DiO (Invitrogen D3898) having a concentration of 1 mg/ml in Milli-Q water. In addition to these Calcium green (Invitrogen C-3732) and Fluo-4 (Invitrogen F-14217) were also used as supplied. Finally, a fluorescent sample, consisting of conventional red water paint (slightly diluted in water) was applied onto a zero thickness cover glass. The dried sample was placed directly at the sample plane of the microscope. The emitted fluorescent spectrum had a bandwidth of 40 nm (measured at the full width half maximum) and was centered at 600nm.

For *in vivo* studies *C. elegans* nematodes expressing GFP in D-Type motoneurons (juIs76 [unc-25::gfp]) were used to perform the imaging experiments. Its transparency and easiness of lab maintenance make this model organism highly attractive for microscopy studies [28]. The strain was grown in nematode growth media and feed with OP50 (*Escherichia coli*). Adult worms were anesthetized using 0.8 µl of 25-mM sodium azide (NaN_3) and mounted on a 2% agar pad sandwiched between two cover glasses (No. 1 - 0.13 to 0.16 mm). The preparations were sealed using melted paraffin and were imaged at room temperature.

#139905 - $15.00 USD Received 21 Dec 2010; revised 23 Feb 2011; accepted 24 Feb 2011; published 28 Feb 2011

3. Results and discussion

The capability of the modelocked SDL for TPEF imaging purposes was first tested employing fixed samples stained with different dyes that are excited at different wavelengths [29] (see Fig. 2). These were 1 μm fluorescent beads (Fig. 2a) and a mouse intestine section (Fig. 2b). To obtain these images the average power excitation, measured at the sample plane, was of ~10 mW.

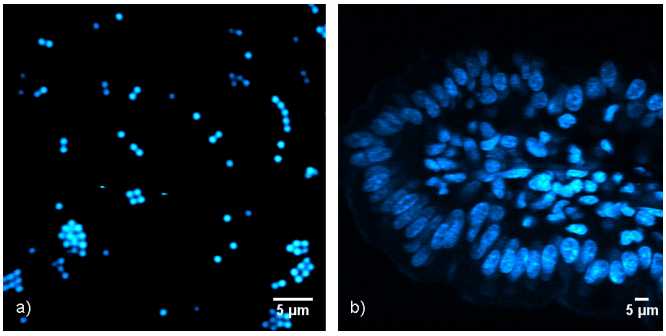

Fig. 2. TPEF images from a) green fluorescent beads and b) mouse intestine section labeled with Alexa Fluor 350 WGA (mucus of goblet cells), Alexa Fluor 568 phalloidin (filamentous actin prevalent in the brush border), and SYTOX Green nucleic acid stain (nuclei of goblet cells). All the images are 500x500 pixels.

The beads shown in Fig. 2a containing green fluorescing firefly dye can be excited at 468nm and therefore these are very efficiently imaged with our laser. From image 2b it is possible to see the nuclei of goblet cells labeled with SYTOX green, and the border surrounding these cells arrangement labeled with Alexa Fluor 568 phalloidin. In this sample, SYTOX green possess an absorption peak at 940 nm. This is very close to the operating wavelength of our laser and therefore, cells are visualized very efficiently. For the cell structure labeled with Alexa fluor 568 (filamentous actin in the brush border) the image region is very faintly observed as the dye is more efficiently excited in the 720-840 nm wavelength range. Finally, for the cells labeled with Alexa Fluor 350 (mucus of goblet cells) there is no TPEF signal observed as the excitation wavelength range is restricted to the 720 - 800 nm.

We then proceed to test the laser for *in vivo* imaging. For this purpose we employed genetically modified *C. elegans* nematodes expressing GFP in VD-Type motoneurons and pharyngeal nerve ring neurons. Furthermore, to emphasize the imaging capabilities of the SDL all the TPEF images where simultaneously recorded with any SHG signal that could be originated from the nematode. Sample imaging was performed employing an average power of 34 mW (measured at the sample plane) which corresponds to a peak power of ~0.04 KW and a FOM_{2p} = 1.5 W^2. Employing this configuration, no damage at the sample was observed. In our setup, the peak power threshold for getting a TPEF image from the GFP expressed in the nematode was ~0.01KW, corresponding to a FOM_{2p} of approximately 0.1 W^2.

The first region to be imaged was the head of an adult *C. elegans* nematode (see Fig. 3). Figure 3a (TPEF signal depicted in blue), shows the 3D projection of the GFP tagged neurons in the *C. elegans* pharyngeal region. Image 3b (SHG signal depicted in orange) shows the anterior bulb of the pharyngeal region. In this figure, some parts of the neurons forming the nerve ring are also observed even though a narrow band SHG filter was used (see materials and methods). This could be possibly due to fluorescence leaking through the SHG filter or SHG emission from the neuron [30]. Mapping the TPEF and SHG signals (Fig. 3c) enables the observation of how the neurons forming the nerve ring innervate with the isthmus of the pharynx.

#139905 - $15.00 USD Received 21 Dec 2010; revised 23 Feb 2011; accepted 24 Feb 2011; published 28 Feb 2011

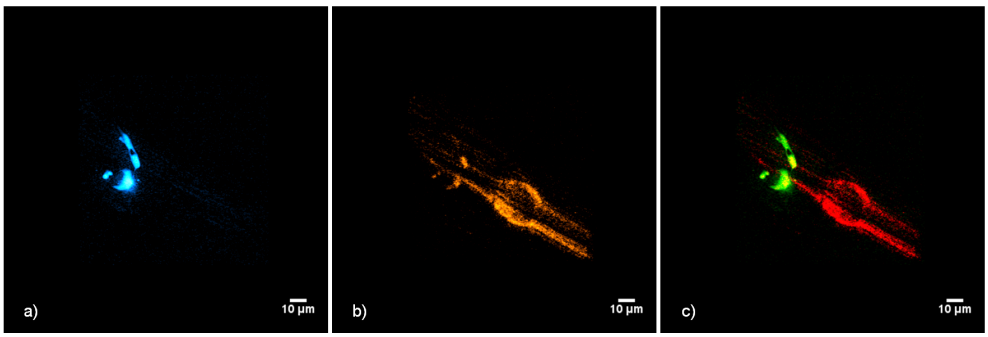

Fig. 3. 3D projections of a) TPEF signal from neurons forming the nerve ring expressing GFP (blue) and b) SHG signal from the pharyngeal region (orange) of the *C. elegans* nematode. c) Merged TPEF (Green) and SHG (red) images of both structures. The 3D projection is composed of 55 stacks separated 1 µm. A single XY optical section was taken in less than 2 seconds. For the SHG image an average of 10 frames was applied to improve the signal to noise ratio. All the images are 500x500 pixels

To further demonstrate the capabilities of this laser we then proceeded to image an adult *C. elegans* nematode near the vulva (see Fig. 4). Figure 4a shows a set of VD-type motoneurons expressing GFP. On the upper part of image 4a, the ventral nerve cord and motoneurons cell bodies (near the vulva) can be clearly observed (bright spots at the top end of the image). Additionally, in the same image on the lower and upper parts, a weak epi-detected SHG signal from body wall and vulval muscles is observed (see green arrows Fig. 4a).

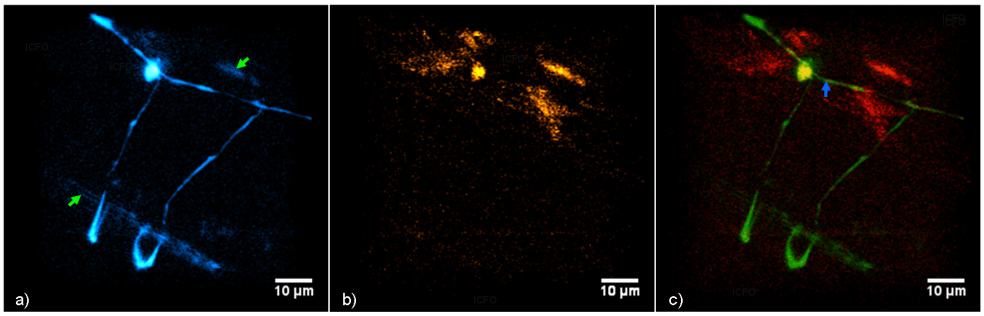

Fig. 4. 3D projections of a) TPEF (blue) of a set of motoneurons expressing GFP and b) SHG (orange) signal of the muscles in the vulval region in a *C. elegans* mid body region. c) Merged TPEF (Green) and SHG (red) images. The 3D projection is composed of 50 stacks separated 1 µm. A single XY optical section was taken in less than 2 seconds. For the SHG image an average of 10 frames was applied to improve the signal to noise ratio. All the images are 500x500 pixels.

In panel 4b, the vulval muscles (*C. elegans* diagonally positioned) can be observed together with a motoneuron cell body (bright spot). This spot, similarly to Fig. 3b, could be due to autofluorescence leaking through the filter or SHG emission by the same motoneuron observed in Fig. 4a. The superposition of both signals enables the observation of the vm-type 1 and 2 vulval muscles and a portion of the body wall muscles in close relation with the motoneurons that are responsible for locomotion (blue arrow).

Based on both imaged regions, we observe a very efficient TPEF signal despite the fact that we are using a very low peak power. The main reason for this is that the employed wavelength is located around GFP maximum of its two-photon action cross-section [2, 27–27]. Furthermore, the relaxation of the required intensities to excite GFP, would, in principle, maximize sample viability given that the ratio of the energy absorbed to the input energy flux determines the possible induced sample damage.

#139905 - $15.00 USD Received 21 Dec 2010; revised 23 Feb 2011; accepted 24 Feb 2011; published 28 Feb 2011

Finally, the use of this laser for TPEF imaging was assessed with other markers. To do so, different dyes (available in our lab) in solutions were excited with a constant laser output power of ~10 mW (measured at the sample plane). Then the relative two-photon signal intensities were recorded using the PMT voltage value. For each image the background signal was first set to zero and then the emitted signal was adjusted so that only a few pixels were saturated (with an intensity of 255). In each case, low TPEF signal resulted in high PMT voltages and vice versa [31]. Figure 5 shows images of the edge of drops of different dyes that were placed on top of a cover glass. In each image, the voltages resulting from the excitation with the SDL laser system were recorded. It is important to mention that, the precise detector setting may vary not only between instruments but also between samples. However the excitation/emission general trend should not change, meaning that the PMT values shown here are not absolute but they are relative guides to help in understanding the imaging capabilities of our laser.

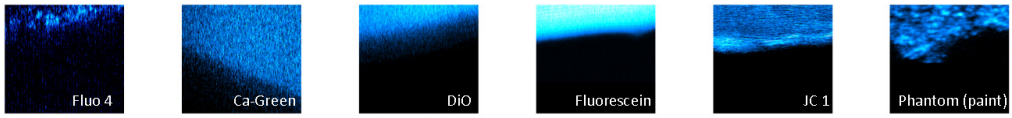

Fig. 5. TPEF images from different dyes in solution. All the images are 500x500 pixels. PMT voltages are Fluo 4: 819 V, Ca-Green: 757 V, DiO: 711 V, Fluorescein: 510 V, JC1: 478 V and Phantom (paint): 572 V. The field of view of all the images is of 40x40 μm.

From above we can observe that the laser can be used for exciting different biological markers. To further illustrate its applicability for these purposes, we have theoretically estimated how efficiently the laser would excite other dyes. Our calculations were based on the two-photon action cross-section of other dyes relative to GFP at 965 nm (~180 GM) for different markers (data taken from ref. 27). By performing such calculation it is possible to determine that the expected TPEF signal compared to GFP are 0.05 for Bodipy, 0.20 for Alexa 488, 0.47 for dsRed. 1.00 for mVenus, 1.15 for YFP, and 1.54 for mCitrine

Alternative applications in which the laser can be used for targeting GFP are monitoring membrane potential [32], selective non-linear optical sensing of electrophysiological processes in *C. elegans* [33] and protein dynamics recording inside living cells through photobleaching experiments [34], just to mention a few.

4. Conclusions

We have successfully demonstrated, for the first time, to the best of our knowledge, the potential use of an ultrafast semiconductor pulsed disk laser (or VECSELs) [20], with a pulse duration of 1.5 ps, average output power of 287 mW and repetition rate of 500 MHz for nonlinear imaging of living *C. elegans* samples expressing GFP, one of the most widely used fluorescent markers.

For instance, the compact design of this laser, having a footprint of only 140x240x70 mm combines a simple and maintenance free operation, as no alignment, cleaning or specialized knowledge is required to operate this laser. Its novel mode-locking mechanism, based on a quantum-dot SESAM, enables to have a self-starting pulsed output immediately after the laser is switched on.

The laser's operating wavelength centered at 965 nm, offers several benefits. Besides inheriting all the advantages of NLM, this laser enables a very efficient TPEF signal excitation as the GFP two-photon action cross section maxima falls around this operating wavelength. This results in extremely efficient generation of images with a very small light dose (~0.04KW peak power and 34 mW average power at the sample) which should be important for preserving the sample viability. This is demonstrated by presenting *in-vivo* TPEF images of *C. elegans* nematodes expressing GFP in a set of motoneurons. As this laser is used for nonlinear imaging, the enhanced signal to noise collection should enable larger penetration depths, reduced production of auto fluorescence from endogenous molecules and slower photo-bleaching rates compared to CLSM.

#139905 - $15.00 USD Received 21 Dec 2010; revised 23 Feb 2011; accepted 24 Feb 2011; published 28 Feb 2011

Finally, the extended versatility of the laser is demonstrated by presenting *in vivo* SHG images of pharynx, uterus and body wall muscles. In addition, a collection of other TPEF images of fixed and bulk dyes (i.e. not based on GFP) was presented. Given this, the employed laser source has the potential to cover a wide range of biological applications not only based on GFP marking but also to include several commonly used fluorescent dyes. This non expensive, turn-key, compact laser system could be used as a platform to develop multimodal microscopes [35] and portable nonlinear bio-imaging devices for clinical studies, facilitating its wide-spread adoption in "real-life" applications.

Acknowledgments

We would like to thank Dr. Joe Culotti (Samuel Lunenfeld Research Institute, in Toronto) for providing the *C. elegans* strain employed for this experiments and César Alonso-Ortega for its maintenance at ICFO. This work is supported by the EU projects FAST DOT (FP7-ICT-2007-2, 224338) and STELUM (FP7-PEOPLE-2007-3-1-IAPP, 217997). Authors also acknowledge The Laser Lab Europe (optobio) and the Photonics4Life Networks of Excellence, the Generalitat de Catalunya grant 2009-SGR-159, the Spanish government grants TEC2009-09698. This research has been partially supported by Fundació Cellex Barcelona.

#139905 - $15.00 USD Received 21 Dec 2010; revised 23 Feb 2011; accepted 24 Feb 2011; published 28 Feb 2011